

Rapid Quantification of Human *ABCA1* mRNA in Various Cell Types and Tissues by Real-Time Reverse Transcription-PCR

DANUTA KIELAR,^{1,3} WOLFGANG DIETMAIER,² THOMAS LANGMANN,¹
CHARALAMPOS ASLANIDIS,¹ MARIO PROBST,¹ MAREK NARUSZEWICZ,³ and GERD SCHMITZ^{1*}

Background: The *ABCA1* gene encodes for a member of subfamily A of the ATP-binding cassette transporters that plays an important role in cellular export of cholesterol and phospholipids; therefore, quantification of the *ABCA1* mRNA is critical in many studies related to its expression and regulation by metabolic factors, nutritional status, and new antiatherogenic drug candidates. We developed a rapid, sensitive, specific, and reproducible real-time reverse transcription-PCR (RT-PCR) method for detection and quantification of *ABCA1* transcripts in total RNA isolated from cultured human cells and tissues.

Methods: To quantify *ABCA1* mRNA, we generated a calibration curve from serial dilutions of in vitro-transcribed RNA corresponding to an amplified *ABCA1* cDNA 205-bp fragment (homologous calibrator). Two pairs of fluorescent hybridization probes were used to detect the *ABCA1* and porphobilinogen deaminase (*PBGD*) mRNAs; the latter served as an internal control. PCR was performed as real-time amplification of *ABCA1* mRNA in 100 ng of total RNA isolated from various human tissues, and cultured cells were calculated from the calibration curve. In addition, normalized values of target (*ABCA1/PBGD* ratio) were calculated.

Results: Using this method, we quantified *ABCA1* transcripts in various human tissue samples as well as in monocytes, THP-1 cells, fibroblasts, and adipocytes. We demonstrated *ABCA1* mRNA up-regulation during human adipocyte and monocyte differentiation. In addition,

we examined the effect of cholesterol loading and deloading on *ABCA1* expression in monocytes, THP-1 cells, and fibroblasts.

Conclusions: Our RT-PCR assay allows the specific and highly reproducible detection and quantification of minute amounts of human *ABCA1* mRNA. This new method is more accurate, more informative, and less laborious than the classic RT-PCR methods and Northern blot; it therefore could simplify all studies on *ABCA1* mRNA expression.

© 2001 American Association for Clinical Chemistry

Cholesterol homeostasis in biologic systems and individual cells is maintained by mechanisms regulating its synthesis, transport, and degradation. The latter process takes place in the liver where it is metabolized to bile acids and subsequently excreted. From peripheral tissues, cholesterol is transported by HDL particles, which protect cells, especially arterial wall macrophages, against sterol overload, a well-known causative factor in atherogenesis. ATP-binding cassette transporter A1 (*ABCA1*)⁴ is a member of subfamily A of the ATP-binding cassette transporters, which cause familial HDL deficiency syndromes (1–3). Initial evidence that *ABCA1* is involved in cholesterol and phospholipid transport came from experiments in macrophages demonstrating that *ABCA1* expression is sensitive to intracellular cholesterol concentrations (4). *ABCA1* mRNA and protein in human macrophages are up-regulated by cholesterol loading and down-regulated by cholesterol deloading. The biologic importance of *ABCA1* was further substantiated by observations that the absence of *ABCA1* protein in patients

¹ Institute for Clinical Chemistry and Laboratory Medicine and ² Institute of Pathology, University of Regensburg, 93042 Regensburg, Germany.

³ Department of Clinical Biochemistry, Pomeranian Medical Academy, 70-111 Szczecin, Poland.

*Address correspondence to this author at: Institute for Clinical Chemistry, University of Regensburg, Franz-Josef-Strauss-Allee 11, D-93042 Regensburg, Germany. Fax 49-941-944-6202; e-mail gerd.schmitz@klinik.uni-regensburg.de.

Received in revised form September 17, 2001; accepted September 18, 2001.

⁴ Nonstandard abbreviations: *ABCA1*, ATP-binding cassette transporter A1; RT-PCR, reverse transcription-PCR; M-CSF, macrophage colony-stimulating factor; E-LDL, enzymatically modified LDL; *PBGD*, porphobilinogen deaminase; *GAPDH*, glyceraldehyde 3-phosphate dehydrogenase; and Cp, crossing point.

with familial HDL-deficiency syndromes, such as Tangier disease, and knock-out mice lacking *ABCA1* causes intracellular accumulation of cholesteryl esters and markedly reduced lipid efflux (5). As a consequence, Tangier patients have very low HDL concentrations associated either with the classic phenotype (splenomegaly) or with premature atherosclerosis and a higher risk of developing coronary artery disease.

Recent results from overexpression studies have demonstrated the importance of *ABCA1* as a major determinant of HDL-cholesterol concentrations in plasma and in cellular trafficking of cholesterol and choline phospholipids (5, 6). *ABCA1* gene expression is up-regulated by modified LDL (4), cAMP (7, 8), and oxysterols, which act on liver X receptor- α and liver X receptor- β together with the retinoid X receptor (9, 10). Few data are available concerning inhibitory factors of *ABCA1* expression. It was shown that activation of mouse peritoneal macrophages by interferon- γ down-regulated *ABCA1* along with a substantial reduction of apolipoprotein A-I-mediated cholesterol and phospholipid efflux (11). A zinc finger transcription factor (ZNF202) located within a hypoalphalipoproteinemia locus on chromosome 11q23 acts as a strong repressor on *ABCA1* expression and cellular lipid efflux (12).

Quantification of *ABCA1* gene expression is critical in studies related to its expression and regulation by metabolic factors, nutritional status, and new antiatherogenic drug candidates. Here we demonstrate that the homogeneous LightCycler-based real-time reverse transcription-PCR (RT-PCR) technique is a reliable and rapid tool that allows the amplification, detection, and quantification of minute amounts of *ABCA1* mRNA in a variety of tissues and cultured cells in contrast to classic RT-PCR or Northern blot analysis.

Materials and Methods

CELL CULTURE

Monocytes were obtained from healthy normolipidemic volunteers by leukapheresis and were purified by counterflow elutriation. Monocyte purity was >95% as confirmed by fluorescence-activated cell-sorting analysis (FACS; Becton Dickinson). Aliquots containing 1×10^6 /mL of monocytes were cultured in macrophage serum-free medium (Gibco). After 12 h, fresh macrophage medium supplemented with 50 μ g/L human recombinant M-CSF was added (R&D Systems). Human skin fibroblasts were cultured to near confluence in DMEM supplemented with 100 mL/L fetal bovine serum and 10 mL/L minimal essential medium. THP-1 cells were obtained from ATCC; cultured in RPMI 1640 (Sigma) supplemented with 10% fetal calf serum (Gibco), 100 kilounits/L penicillin, and 100 mg/L streptomycin; and incubated in 10% CO₂ in air at 37 °C. Human subcutaneous preadipocytes and adipocytes were kindly provided by Dr. Georg Löffler (Institute for Biochemistry, Genetics and Microbiology, University of Regensburg, Germany).

ENZYMATIC MODIFICATION OF LDL

LDL ($d = 1.006$ – 1.063 kg/L) and HDL₃ ($d = 1.125$ – 1.21 kg/L) were prepared from human plasma of healthy donors by standard methods (13).

Enzymatic modification of LDL was performed as described (14–16). Briefly, LDL was diluted to 2 g/L of protein in HEPES buffer (20 mmol/L HEPES, 150 mmol/L NaCl, 2 mmol/L CaCl₂, pH 7.0). Enzyme treatment was with trypsin (6.6 g/L; Sigma) and cholesterol esterase (40 g/L; Roche Biochemica) for 6–8 h at 37 °C. Subsequently, trypsin inhibitor (Sigma) was added, and the pH of the solution was adjusted to 5.5 by the addition of MES buffer, pH 5.0.

Table 1. Primers and hybridization probes used to detect *ABCA1* and *PBGD* transcripts.

Oligonucleotides ^a	Position ^b in message	GC, %	Length, nt
<i>ABCA1</i>			
Forward primer: GCACTGAGGAAGATGCTGAAA	1327	47.6	21
Reverse primer: AGTTCCTGGAAGGTCTTGTTCAC	1532	47.8	23
Donor probe: GCCGCTGCTCGTTGGGAAGAT-flu ^c	1068	61.9	21
Acceptor probe: LCRed 640-CTGTATACACTGACACTCCAG-ph	1090	50.0	22
<i>PBGD</i>			
Forward primer: GAGTGATTCGCGTGGGTACC	85	57.1	21
Reverse primer: GGCTCCGATGGTGAAGCC	349	66.7	18
Donor probe: AGTGGACCTGGTTGTGCACTCCTTGAA-flu	297	48.1	28
Acceptor probe: LCRed 640-ACCTGCCACTGTGCTTCCTCT-ph	326	60.9	23
<i>GAPDH</i>			
Forward primer: TTGGTATCGTGAAGGACTCA	504	47.6	21
Reverse primer: TGTCATCATATTTGGCAGGTTT	753	36.4	22
Donor probe: TGTCCCACTGCCAACGTGTCAG-flu	703	60.9	23
Acceptor probe: LCRed 640-GGTGGACCTGACCTGCCGTCTAGA-ph	727	62.5	24

^a Oligonucleotide sequences are 5' to 3'.

^b Accession numbers: AF275948 (human *ABCA1* mRNA), X04217 (human *PBGD* mRNA), J02642 (human *GAPDH* mRNA).

^c flu, fluorescein; ph, phosphoryl group.

Neuraminidase (79 U/L; Behring) and magnesium ascorbate solution (30 g/L) were then added for 14 h at 37 °C. Subsequently, the solution was neutralized with 1 mol/L NaOH. The absence of oxidation products in the enzymatically modified LDL (E-LDL) was verified by measurement of the thiobarbituric acid-reactive substances to quantify lipid peroxidation products (17). Modified lipoproteins were stored at 4 °C and used within 1 week. During LDL preparation and subsequent modification, general precautions were taken to avoid lipopolysaccharide contamination. The latter was monitored by the *Limulus* endotoxin assay (Kinetic-QCL; BioWhittaker).

RNA ISOLATION

Total RNA from different human tissues was obtained from Clontech. Total RNA from human preadipocytes, adipocytes, fibroblasts, monocytes, macrophages, and THP-1 cells was isolated from in vitro cultures with Trizol reagent (Sigma). All RNA samples were treated with DNase I (Roche) according to the protocol of Huang et al. (18). The concentration, purity, and integrity of the RNA were assessed on the Agilent 2100 bioanalyzer with the RNA 6000 LabChip® reagent set (Agilent Technologies).

GENERATION OF AN EXTERNAL ABCA1 RNA CALIBRATOR

A 205-bp *ABCA1* RT-PCR product was subcloned in the plasmid vector pCR® II-TOPO containing a T7 RNA polymerase promoter (TOPO TA Cloning; Invitrogen) according to the manufacturer's instructions. Plasmid DNA was isolated and purified with the Qiaprep Spin Miniprep Kit (QIAGEN). The *ABCA1* insert sequence was verified by DNA sequencing on an ABI Prism Genetic Analyzer 310 (PE Biosystems). Linearization of purified plasmid DNA was achieved by restriction with *Bam*HI, and RNA was synthesized in vitro with the RiboProbe® In Vitro Transcription System (Promega) and T7 polymerase according to the protocol for large-scale RNA synthesis.

PRIMERS AND HYBRIDIZATION PROBES

ABCA1-specific PCR primers and hybridization probes capable of fluorescence resonance energy transfer were used to generate and monitor 205-bp *ABCA1*, 264-bp porphobilinogen deaminase (*PBGD*) fragments, and 262-bp glyceraldehyde 3-phosphate dehydrogenase (*GAPDH*) fragments, respectively (Table 1). All primers and hybridization probes were synthesized by TIB MOLBIOL. The pairs of hybridization probes were labeled with fluorescein at their 3' ends (donor probes) and with LC-Red 640 at their 5' ends (acceptor probes).

RT-PCR

First-strand cDNA synthesis was performed in a total volume of 20 µL containing 40 U of AMV Reverse Transcriptase, 2.0 µL of 10× Reaction Buffer, 50 units of RNase Inhibitor, 2 µL of Deoxynucleotide Mix (1 mM), 2 µL of Random Primer p(dN)₆ (3.2 µg), 4 µL of MgCl₂ (5 mM), and 1 µg of total RNA, as recommended by the manufacturer [1st Strand cDNA Synthesis Kit for RT-PCR (AMV); Roche Molecular Biochemicals]. Serial dilutions of in vitro-synthesized *ABCA1* RNA (100, 10, 1, and 0.1 pg) were reverse-transcribed, and 1/10 of each reaction was used for generation of a calibration curve (Fig. 2). After cDNA synthesis for 60 min at 42 °C and inactivation of the enzyme at 95 °C for 5 min, PCR reactions were performed in the LightCycler instrument with the FastStart DNA Master Hybridization Probes Kit (Roche Molecular Biochemicals). Each reaction mixture consisted of 2 µL of cDNA from the reverse transcription step (unknown samples and each dilution of the calibrator), a pair of flanking PCR primers (0.5 µM each), two pairs of acceptor and detection probes (0.3 µM each), 1.5 µL of "Hot Start" PCR Reaction Mix, 2.4 µL of 25 mM MgCl₂, and PCR-grade water up to a final volume of 15 µL. For all samples, a master mixture was prepared, and 13 µL was transferred into each precooled glass capillary. cDNA (2 µL) was then pipetted into all but one of the capillaries; 2 µL of PCR-grade water was added to that capillary as a negative control. Denaturation was performed at 95 °C for 10 min, followed by 45 PCR cycles of 95 °C for 10 s, annealing at 60 °C for 10 s, and elongation at 72 °C for 5 s in the glass capillaries. For quantification, an external homologous *ABCA1* RNA calibrator was generated as described above. The calibration curve (Fig. 2B) was used to quantify both target mRNAs, *ABCA1* and *PBGD*. Both absolute (pg *ABCA1*/sample) and normalized (*ABCA1*/*PBGD* ratio) values for the target gene were calculated. The data are means of at least three independent measurements. For the efficiency analysis of the target (*ABCA1*) and control genes (*PBGD* and *GAPDH*), cDNA from macrophages was serially diluted in 1:10 steps and amplified in the LightCycler by the same protocol. Crossing point (Cp) cycles vs cDNA dilution input were plotted to calculate the slope. The corresponding real-time PCR efficiencies (*E*) for each *PBGD*, *GAPDH*, and *ABCA1* assay were calculated according to the equation: $E = 10^{(-1/\text{slope})}$ (Fig. 3).

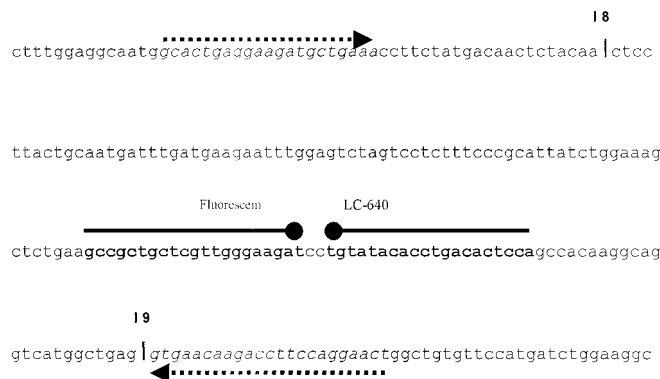


Fig. 1. Locations of *ABCA1* PCR primers and hybridization probes. A pair of primers (dotted arrows) amplify a 205-bp fragment of the *ABCA1* cDNA containing a part of exon 8, all of exon 9, and the first 23 bp of exon 10 (position in *ABCA1* mRNA, bp 1327–1532 in accession number AF275948). The *ABCA1* donor hybridization probe and *ABCA1* acceptor hybridization probe (solid lines) are separated by two nucleotides. Positions of introns 8 (2.7 kb) and 9 (0.3 kb) are shown by vertical lines.

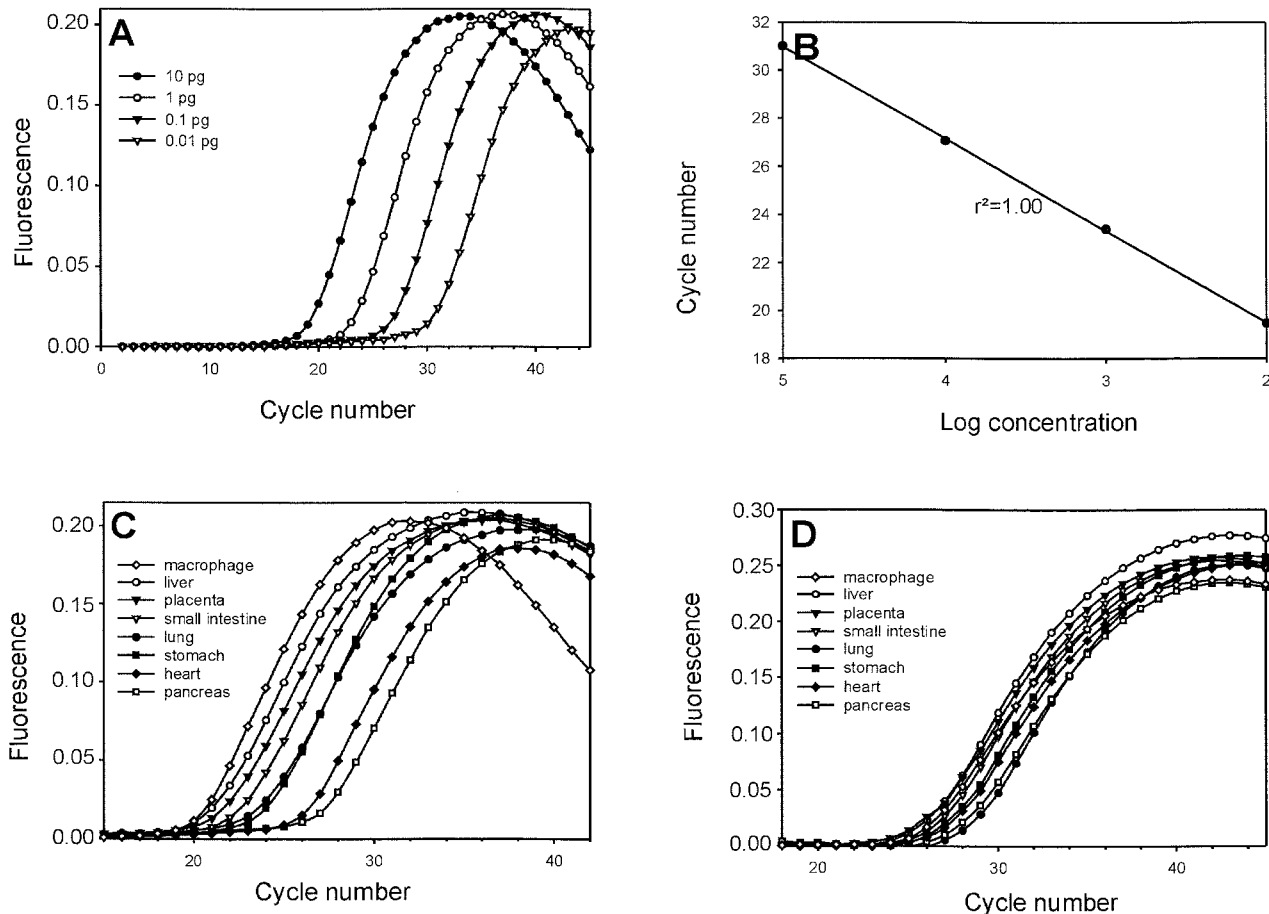


Fig. 2. Detection and monitoring of *ABCA1* product amplified in the LightCycler using the Hybridization Probe Format.

Serial dilutions (100, 10, 1, 0.1 pg) of the in vitro-transcribed *ABCA1* cRNA fragment (external standard) were first reverse transcribed; 1/10 of each reverse transcription reaction mixture (10, 1, 0.1, 0.01 pg) was amplified (A) to generate a calibration curve (B) for absolute *ABCA1* and *PBGD* transcript quantification [y -intercept = 11.85 [log of the amount of PCR product at the Cp divided by the log of E ($E = 10^{(-1/\text{slope})} = 10^{(-1/-3.826)} = 1.82$)]; slope = -3.826 ($-1/\log E$); error = 0.0165 (mean squared error); regression coefficient (r^2) = 1.00]. The Cp values of the unknown samples are converted to concentrations based on the equation derived from the calibrator. Depending on the initial concentrations of *ABCA1* (C) and *PBGD* (D) in unknown samples, increases in signal intensity become detectable (threshold cycle) at different cycles.

NORTHERN BLOT ANALYSIS

Total RNA (10 μg) isolated from macrophages of three healthy donors and from all human tissues analyzed by real-time PCR was separated on a 1.2% agarose-formaldehyde gel and transferred to a nylon membrane (Schleicher & Schuell) followed by ultraviolet cross-linking (Stratalinker Model 1800; Stratagene). For detection of *ABCA1* mRNA, the membranes were hybridized with a 1-kb *ABCA1* DNA fragment derived from PCR amplification using the primers described by Langmann et al. (4). The same membranes were reprobated with *GAPDH* cDNA.

Results

To amplify a human *ABCA1*-specific 205-bp RT-PCR fragment, we designed PCR primers located in the 3' part of exon 8 and at the beginning of exon 10, respectively. As shown in Fig. 1, these primers span across introns 8 and 9, preventing the amplification of genomic DNA templates. The hybridization probes are separated by two nucleotides

and are complementary to the sequence within the central region of exon 9. *ABCA1* mRNA expression was normalized using specific primers and hybridization probes for a 264-bp *PBGD* fragment. In addition, for efficiency analysis, specific primers and hybridization probes that detect human *GAPDH* were used. The primer and hybridization probe sequences and characteristics for *ABCA1*, *PBGD*, and *GAPDH* are shown in Table 1. Efficiency analysis for the target (*ABCA1*) and two housekeeping genes (*PBGD* and *GAPDH*; Fig. 3) showed that only *PBGD* had an amplification efficiency very similar to that of *ABCA1* (1.82 and 1.80, respectively); therefore, *PBGD* was used in our assay instead of the commonly used *GAPDH*, which had a higher amplification efficiency here ($E = 2.00$).

To achieve absolute quantification of *ABCA1* mRNA, we used serially diluted homologous in vitro-transcribed *ABCA1* RNA as an external control. Four dilutions of *ABCA1* cRNA were reverse transcribed in parallel to the sample material to be analyzed, and 2 μL of each reverse

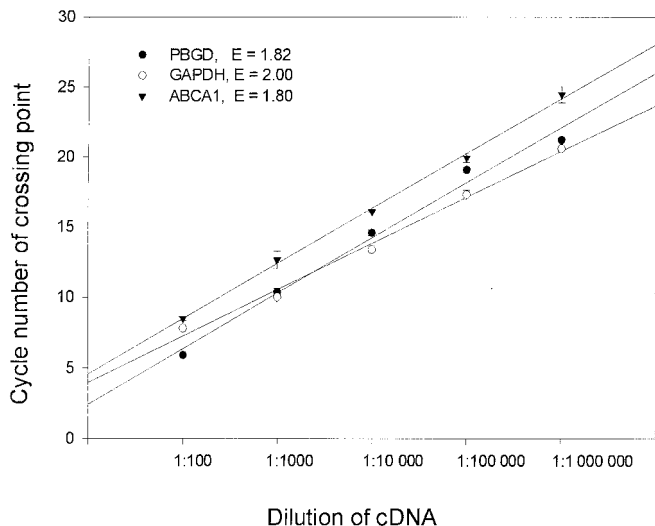


Fig. 3. Quantitative PCR of titrated cDNA samples for efficiency (*E*) analysis.

cDNA from macrophages was serially diluted in 1:10 steps and amplified with specific primers and hybridization probes to estimate and compare efficiencies of the target gene (*ABCA1*) and the control genes (*PBGD* and *GAPDH*). Cp cycles vs cDNA dilutions input were plotted to calculate the slope (mean \pm SD; $n = 3$). The corresponding real-time PCR efficiencies were calculated according to the equation: $E = 10^{(-1/\text{slope})}$.

transcription reaction was amplified with the probes for *ABCA1* and *PBGD* in the LightCycler. The real-time PCR curves from the amplification of the *ABCA1* cRNA dilutions that were used to generate the calibration curve are displayed in Fig. 2A. The calibration curve (Fig. 2B) was used for quantification of both the *ABCA1* transcript and the housekeeping gene (*PBGD*) when relative quantities were calculated. In contrast to *GAPDH*, *PBGD* was amplified with the same efficiency as the target *ABCA1* gene (Fig. 3) and therefore was chosen as the internal standard. One aliquot of cDNA was used to analyze *ABCA1* in each sample, whereas we used another aliquot to determine *PBGD* expression. Both transcripts were amplified simultaneously during the same run. Depending on the initial

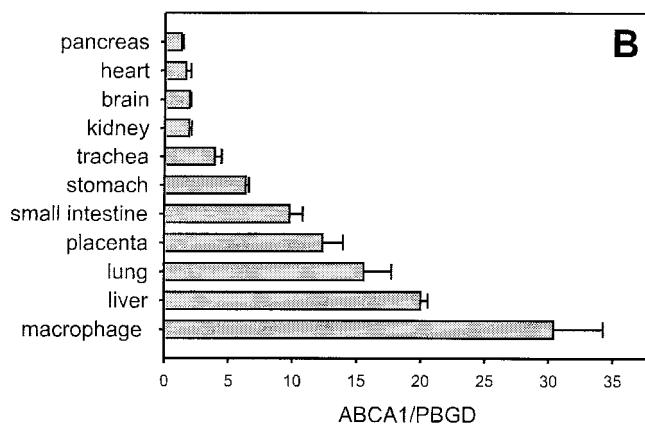
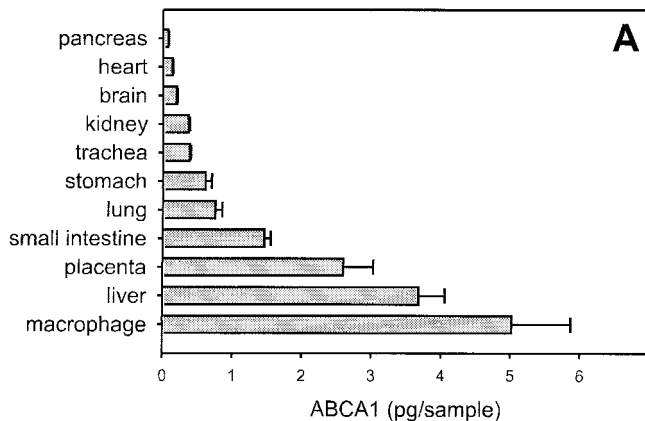


Fig. 5. *ABCA1* mRNA expression in human tissues.

Total RNA (1 μ g) from each tissue was reverse transcribed, and 2- μ L aliquots of the reverse transcription reaction mixtures were amplified in the presence of hybridization probes. The absolute amounts (pg/sample) of *ABCA1* transcripts were calculated as described in the legend for Fig. 2. *ABCA1/PBGD* ratios were calculated by dividing the absolute amounts of *ABCA1* and *PBGD* determined for each sample. Columns represent mean values (error bars, \pm SD) of four independent measurements. (A), absolute amounts (pg/sample) of *ABCA1* transcript; (B), *ABCA1/PBGD* ratios.

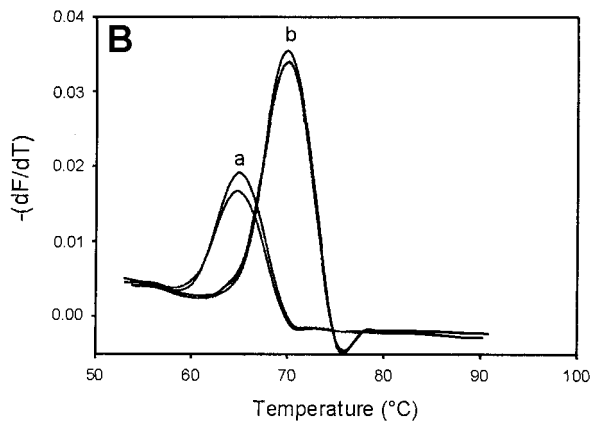
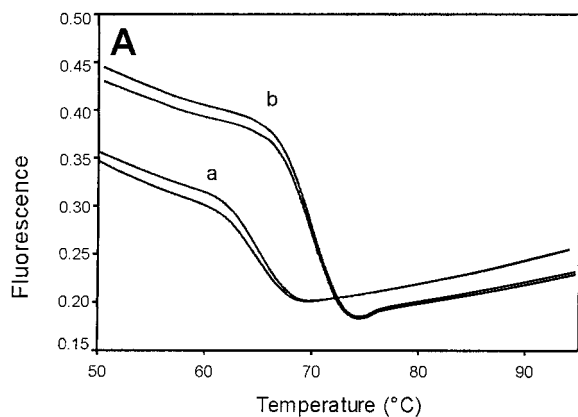


Fig. 4. Melting curves (A) and melting peaks (B) of *ABCA1* (a) and *PBGD* (b) PCR products.

Melting curves (A) were converted to melting peaks (B) by plotting the first negative derivative of the fluorescence with respect to the temperature ($-dF/dT$) against the temperature. Melting temperatures (T_m) characterize each of the products *ABCA1* (a) and *PBGD* (b), respectively.

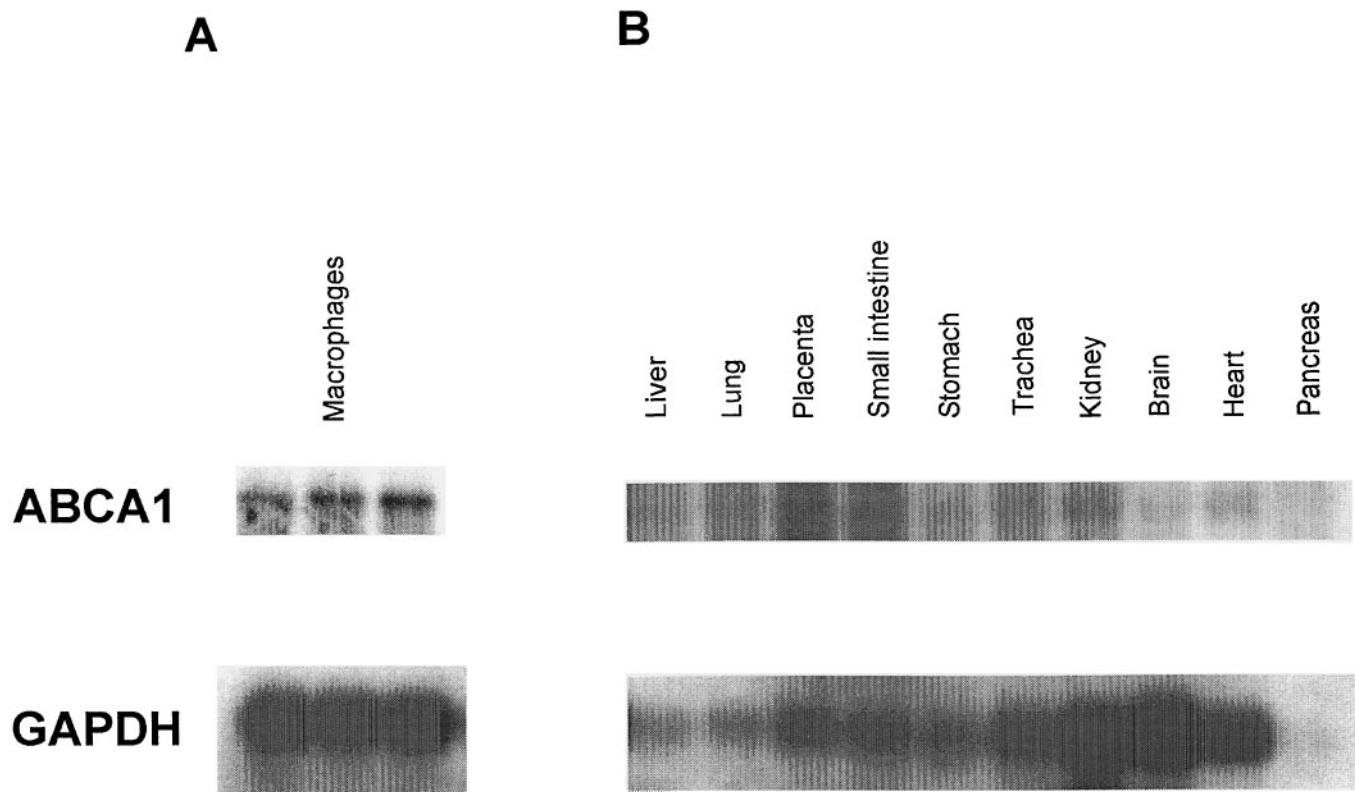


Fig. 6. Northern blot analysis of *ABCA1* and *GAPDH* expression in various human tissues.

Total RNA (10 μ g) isolated from macrophages from three healthy donors (A) and from all human tissues analyzed by real-time PCR (B) was separated on a 1.2% agarose-formaldehyde gel and transferred to a nylon membrane. For detection of *ABCA1* mRNA, the membranes were hybridized with a 1-kb cDNA fragment derived from PCR amplification. The same membranes were reprobed with *GAPDH* cDNA.

concentration of target mRNA, signal intensity began to increase at different cycles. Amplification profiles for the *ABCA1* and *PBGD* targets in various human tissues are shown in Fig. 2, C and D, respectively. The initial template concentration was calculated by LightCycler software based on the cycle at which the fluorescent signal crossed a threshold in the exponential phase of the PCR reactions (Cp). To characterize the amplified products, melting curves (Fig. 4A) were generated for all samples after each run and then converted into melting peaks (Fig. 4B). The melting points (T_m) identified and discriminated between both analyzed products (64.6 and 69.8 $^{\circ}$ C for *ABCA1* and *PBGD*, respectively).

ABCA1 mRNA expression in various tissues compared with macrophages is shown in Fig. 5. The results shown in Fig. 5A are absolute amounts of *ABCA1* mRNA based on a calculation using the calibration curve (pg/sample), whereas the results shown in Fig. 5B are standardized by the quantification of *PBGD*. From all samples examined, the highest amounts of *ABCA1* mRNA were found in macrophages loaded with E-LDL, followed by liver, lung, placenta, small intestine, and stomach. The lowest amounts of *ABCA1* transcripts were detected in pancreas and heart. Fig. 6 shows the Northern blot analysis of *ABCA1* mRNA in macrophages from three healthy donors (Fig. 6A) and from all human tissues analyzed by real-time PCR (Fig. 6B).

Except for macrophages, the amount of *ABCA1* mRNA in human tissues was rather low when analyzed with this method; therefore, long-term exposure of the x-ray film was necessary (1 week; Fig. 6B). For macrophages, overnight exposure was sufficient. Rehybridization with the *GAPDH* cDNA commonly used for Northern blot analysis revealed variable expression of *GAPDH* in different tissues; nevertheless, the expression was constant in macrophages in different individuals (Fig. 6A).

To examine the effect of monocyte differentiation on *ABCA1* expression, we cultured freshly isolated monocytes in vitro for 4 days in serum-free medium supplemented with M-CSF (Fig. 7A). To examine the effect of E-LDL on *ABCA1* mRNA concentrations, we incubated differentiated monocytes (Fig. 7A) and THP-1 cells (Fig. 7B) for 2 days in the presence or absence of E-LDL (40 mg/L). In addition to the up-regulation of *ABCA1* during differentiation, cholesterol loading (E-LDL) induced *ABCA1* expression in both cell types (Fig. 7, A and B). Expression of *ABCA1* mRNA in normal human fibroblasts (Fig. 7C) was measured under basal conditions and after incubation with HDL₃ (100 mg/L) for 1 and 12 h, respectively. We could demonstrate that a 12-h incubation of fibroblasts with HDL₃ (cholesterol deloading) caused a substantial decrease in *ABCA1* mRNA expression.

Unlike macrophages, adipocytes store cholesterol

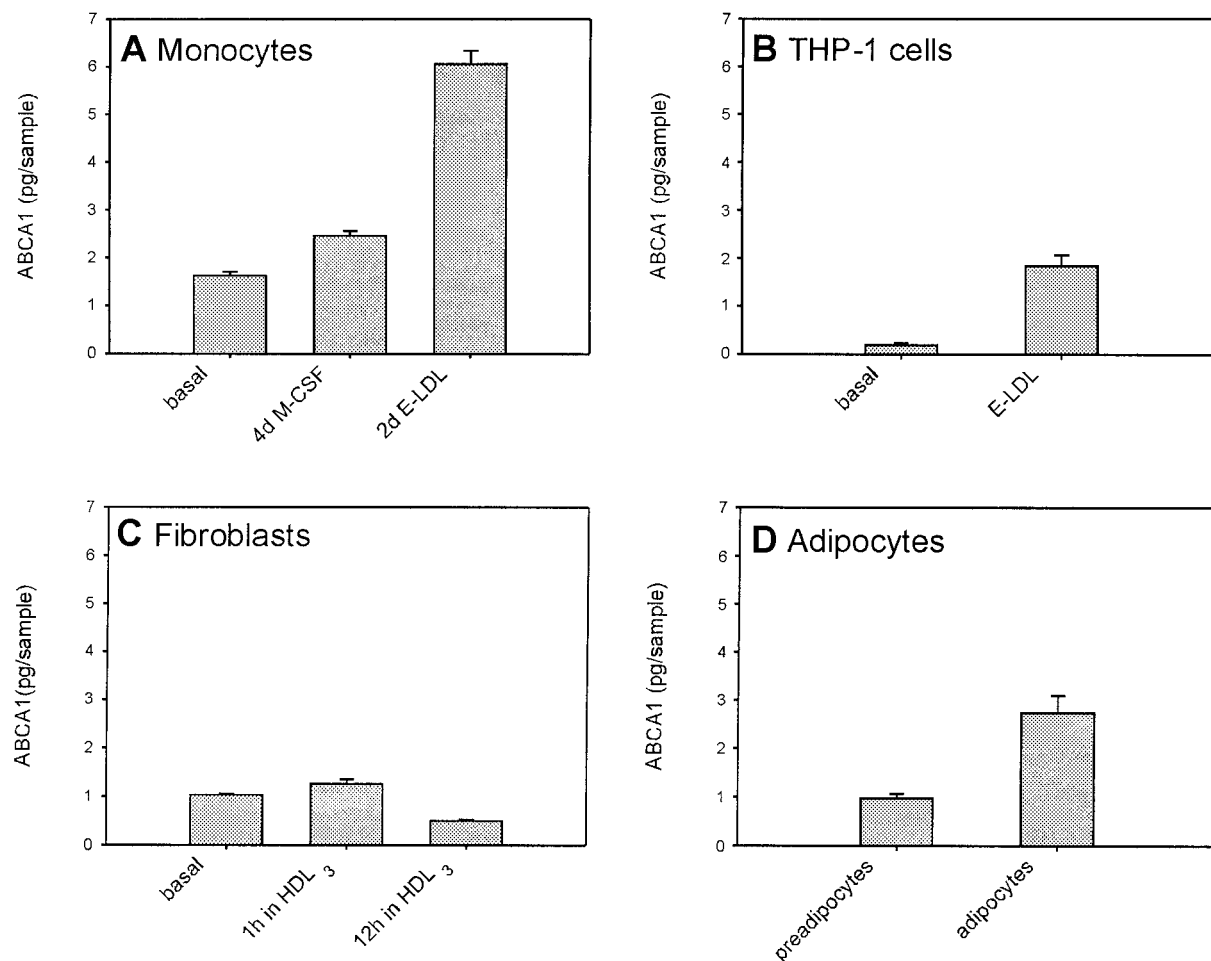


Fig. 7. Expression of *ABCA1* transcripts in human monocytes (A), THP-1 cells (B), human fibroblasts (C), and human adipocytes (D) after incubation with M-CSF and E-LDL.

Total RNA from all cells was isolated as described in *Materials and Methods*. RT-PCR and quantification were performed by real-time PCR. (A), human monocytes were incubated for 4 days in culture with M-CSF and were cultured for 2 days in the absence (*basal*) or presence of E-LDL (40 mg/L). (B), THP-1 cells were incubated with or without (*basal*) E-LDL. (C), human fibroblasts were cultured in the absence of HDL₃ (*basal*) or for 1 or 12 h with HDL₃ (100 mg/L). *ABCA1* expression was measured in skin fibroblasts from a Tangier patient. In addition, human preadipocytes and adipocytes were analyzed for *ABCA1* expression (D). Amounts of *ABCA1* mRNA were determined as described in the legend for Fig. 2. Columns represent mean values (error bars, \pm SD) of four independent measurements, expressed in pg/sample.

mainly in the unesterified form (19). Cholesterol accumulation increases during differentiation, which is paralleled by an increase in triglyceride content (20). We were interested to see whether *ABCA1* was expressed in adipocytes and whether there was a differentiation-dependent component in its regulation. Fig. 7D shows a substantially higher amount of *ABCA1* transcripts in differentiated human subcutaneous adipocytes compared with preadipocytes. To our knowledge, this is the first study reporting on the detection and differentiation-dependent up-regulation of *ABCA1* mRNA in human subcutaneous preadipocytes and adipocytes.

Discussion

The findings that *ABCA1* is a major player in reverse cholesterol transport renders this protein an interesting drug target for the treatment of atherosclerosis. Therefore, the identification of new pharmacologic agents that reg-

ulate *ABCA1* gene expression and protein synthesis will be a major challenge. Until recently, studies on gene expression have used standard quantification methods, mostly conventional competitive and noncompetitive RT-PCR and Northern blot. These technologies are often time-consuming and not always reliable. In an attempt to measure the absolute expression of human *ABCA1* transcripts in various tissues and cell types, we have established a real-time RT-PCR assay for this gene. Currently there are many RT-PCR quantification strategies available; however, the application of fluorescence techniques that allow on-line monitoring of PCR products during amplification has dramatically improved quantitative analysis. We chose the real-time PCR technology because of its speed, sensitivity, reproducibility, and flexibility regarding probe utility (21, 22). Various probes and dyes are compatible with LightCycler (e.g., DNA-binding dyes, Molecular Beacons, hybridization probes, hydrolysis

probes, and Scorpions). To quantify our targets we applied a sequence-specific detection system with hybridization probe pairs that bound complementarily to *ABCA1* and *PBGD* PCR products, respectively. Alternatively, SYBR Green I could be used, but optimization of PCR conditions is of greater importance because of interfering primer-dimers. In contrast to the end-point analysis of accumulating PCR products in conventional PCR, real-time PCR enables calculation of initial target concentration during the log-linear phase of the PCR reaction based on the fluorescence resonance energy transfer between two adjacent hybridization probes labeled with fluorophores. The advantage of the hybridization probe format is its specificity as confirmed by melting curve analysis for each amplified product, in our case, *ABCA1* and *PBGD* (Fig. 4). The melting points (T_m) for the *ABCA1* and *PBGD* products were 64.6 and 69.8 °C, respectively, and no run-to-run variation was observed. Melting curve analysis at the end of the real-time assay enables characterization of the amplified product and obviates gel electrophoresis.

Among all tissues examined in this study, high *ABCA1* mRNA expression was identified in the liver, placenta, small intestine, and stomach, but the strongest expression was observed in macrophages loaded with E-LDL (Fig. 5). The lowest amount of *ABCA1* transcripts was detected in the pancreas and heart. Tissue expression of *ABCA1* mRNA was previously assessed with conventional technologies, which are less accurate (4). The expression patterns of *ABCA1* mRNA displayed in Fig. 5A (absolute *ABCA1* mRNA) and Fig. 5B (relative amount) show differences. On the basis of the above results, we conclude that standardization with a housekeeping gene (e.g., *PBGD*) is not completely satisfactory when the expression of a target gene (e.g., *ABCA1*) in different tissues and different cells needs to be analyzed. Because *PBGD* is not expressed equally in various tissues, absolute quantification may be more reliable. However, when we normalized the absolute amounts of *ABCA1* mRNA with *PBGD* as a reference gene in the same cell type (e.g., fibroblasts or monocytes), we obtained comparable results. In contrast, the other commonly used internal standard, *GAPDH*, has been demonstrated to vary quantitatively in response to various factors, rendering interpretation of the results difficult (21, 23). The expression of *GAPDH* has also been reported to vary across tissues (24), and it can also be seen in our Northern blot data (Fig. 6B). We rehybridized our Northern blot membrane with *PBGD* cDNA and obtained only very weak signals (data not shown).

Our initial experiments with *GAPDH* as an endogenous control prompted us to use *PBGD* as a reference gene (25). In our hands, unlike *GAPDH* ($E = 2.00$), both *ABCA1* and *PBGD* transcripts were amplified with almost the same efficiency ($E = 1.80$ and 1.82 , respectively; Fig. 3), which is a critical factor for the final calculation of expression values (26). In addition, the amounts of both transcripts expressed were similar, in contrast to *GAPDH*.

Furthermore, unlike for *GAPDH*, no pseudogene has been reported for human *PBGD* (27); thus, only cDNA-derived products are amplified by PCR. This may be a critical factor in cases where DNase digestion after RNA extraction is avoided to minimize loss of material. On the basis of our data, we recommend *PBGD* as a normalization control for mononuclear cells, fibroblasts, adipocytes, HepG2 cells, HeLa cells, and THP-1 cells. When we analyzed RNA samples from liver and lung taken from different individuals, we observed substantial differences in *ABCA1* mRNA expression (data not shown). Because *ABCA1* shows high expression in macrophages, the accumulation of these cells in some tissues under certain conditions, e.g., inflammation, may be responsible for the observed variations in *ABCA1* mRNA expression in these tissues.

As we demonstrated previously by Northern blot analysis (4) and semiquantitative RT-PCR (28), expression of human *ABCA1* mRNA in macrophages is regulated in a differentiation-dependent fashion. Here we confirmed these results with our new quantitative assay (Fig. 7A). E-LDL taken up by human macrophages and smooth muscle cells contributes to the formation of early atherosclerotic lesions (15, 16, 29, 30) and up-regulates *ABCA1* mRNA in macrophages and THP-1 cells. A similar up-regulation of *ABCA1* mRNA has been reported in human monocyte-derived macrophages loaded with acetylated LDL (4, 28). Conversely, cholesterol efflux mediated by HDL₃ down-regulated *ABCA1* expression. We have used fibroblasts and monocytes to confirm this effect of HDL₃ as an exogenous lipid acceptor in down-regulating *ABCA1* mRNA (Fig. 7C). The expression and function of *ABCA1* in adipocytes have been not investigated to date. Adipose tissue serves not only as the main triglyceride storage site in humans, but also represents the largest deposit of unesterified cholesterol (19, 31). The amounts of both lipids increase during adipocyte differentiation, and Prattes et al. (32) recently demonstrated that most of the intracellular pool of free cholesterol in adipocytes is tightly associated with triglyceride droplets where it forms an outer lipid layer. Cholesterol efflux experiments revealed that a triglyceride-associated cholesterol pool is mobilized from these cells when stimulated with extracellular cholesterol acceptors (32). On the basis of those data and our results showing up-regulation of *ABCA1* mRNA during adipocyte differentiation, we suggest that *ABCA1* is involved in cholesterol trafficking in adipocytes.

Our quantitative real-time RT-PCR assay with hybridization probes allowed us to quantify the absolute amounts of *ABCA1* transcripts and to determine the relative expression (*ABCA1*/*PBGD* ratios). This novel assay for the quantification and monitoring of *ABCA1* transcripts is rapid, reliable, highly reproducible, and therefore applicable for (a) monitoring drugs effects, (b) epidemiologic studies, (c) studies assessing correlation between *ABCA1* expression and susceptibility to lipid disorders, and (d) exploring the effects of polymorphisms in the promoter region of the *ABCA1* gene.

This work was supported in part by a grant from Bayer AG. We thank Dr. Löffler (Institute for Biochemistry, Genetics and Microbiology, University of Regensburg, Regensburg, Germany) for providing human adipocytes and preadipocytes.

References

- Bodzioch M, Orsó E, Klucken J, Langmann T, Böttcher A, Diederich W, et al. The gene encoding ATP-binding cassette transporter 1 is mutated in Tangier disease. *Nat Genet* 1999;22:347–51.
- Brooks-Wilson A, Marcil M, Clee SM, Zhang LH, Roomp K, van Dam M, et al. Mutations in ABC1 in Tangier disease and familial high-density lipoprotein deficiency. *Nat Genet* 1999;22:336–45.
- Rust S, Rosier M, Funke H, Real J, Amoura Z, Piette JC, et al. Tangier disease is caused by mutations in the gene encoding ATP-binding cassette transporter 1. *Nat Genet* 1999;22:352–5.
- Langmann T, Klucken J, Reil M, Liebisch G, Luciani MF, Chimini G, et al. Molecular cloning of the human ATP-binding cassette transporter 1 (hABC1): evidence for sterol-dependent regulation in macrophages. *Biochem Biophys Res Commun* 1999;257:29–33.
- Orsó E, Broccardo C, Kaminski WE, Böttcher A, Liebisch G, Drobnik W, et al. Transport of lipids from Golgi to plasma membrane is defective in Tangier disease patients and Abc1-deficient mice. *Nat Genet* 2000;24:192–6.
- Lawn RM, Wade DP, Garvin MR, Wang X, Schwartz K, Porter JG, et al. The Tangier disease gene product ABC1 controls the cellular apolipoprotein-mediated lipid removal pathway. *J Clin Invest* 1999;104:R25–R31.
- Oram JF, Lawn RM, Garver MR, Wade DP. ABCA1 is the cAMP-inducible receptor that mediates cholesterol secretion from macrophages. *J Biol Chem* 2000;275:34508–11.
- Abe-Dohmae S, Suzuki S, Wada Y, Aburatani H, Vance DE, Yokoyama SR. Characterization of apolipoprotein-mediated HDL generation induced by cAMP in a murine macrophage cell line. *Biochemistry* 2000;39:11092–9.
- Costet P, Luo Y, Wang N, Tall AR. Sterol-dependent transactivation of the ABC1 promoter by the liver X receptor/retinoid X receptor. *J Biol Chem* 2000;275:28240–5.
- Repa JJ, Turley SD, Lobaccaro JA, Medina J, Li L, Lustig K, et al. Regulation of absorption and ABC1-mediated efflux of cholesterol by RXR heterodimers. *Science* 2000;289:1524–9.
- Panousis CG, Zuckerman H. Interferon- γ induces downregulation of Tangier disease gene (ATP-binding-cassette transporter 1) in macrophage-derived foam cells. *Arterioscler Thromb Vasc Biol* 2000;20:1565–71.
- Porsch-Özcürümez M, Langmann T, Heimerl S, Borsukova H, Kaminski HW, Drobnik W, et al. The zinc finger protein (ZNF202) is a transcriptional repressor of ABCA1 and ABCG1 gene expression and a modulator of cellular lipid efflux. *J Biol Chem* 2001;276:12427–33.
- Lindgren FT, Adamos GL, Jenson LC, Wood PD. Lipid and lipoprotein measurements in normal adult American population. *Lipids* 1975;10:750–6.
- Bhakdi S, Dorweiler B, Kirchmann R, Torzewski J, Weise E, Trantum-Jensen J, et al. On the pathogenesis of atherosclerosis: enzymatic transformation of human low density lipoprotein to an atherogenic moiety. *J Exp Med* 1995;182:1959–71.
- Torzewski M, Klouche M, Hock J, Messner M, Dorweiler B, Torzewski J, et al. Immunohistochemical demonstration of enzymatically modified human LDL and its colocalization with the terminal complement complex in the early atherosclerotic lesion. *Arterioscler Thromb Vasc Biol* 1998;18:369–78.
- Klouche M, Rose-John S, Schmiedt W, Bhakdi S. Enzymatically degraded, nonoxidized LDL induces human vascular smooth muscle cell activation, foam cell transformation, and proliferation. *Circulation* 2000;101:1799–805.
- Steinbrecher UP, Parthasarathy S, Leake DS, Witztum JL, Steinberg D. Modification of low density lipoprotein by endothelial cells involves lipid peroxidation and degradation of low density lipoprotein phospholipids. *Proc Natl Acad Sci U S A* 1984;81:3883–7.
- Huang Z, Fasco MJ, Kaminsky LS. Optimisation of DNase I removal of contaminating DNA from RNA for use in quantitative RNA-PCR. *Biotechniques* 1996;20:1012–20.
- Krause BR, Hartman D. Adipose tissue and cholesterol metabolism [Review]. *J Lipid Res* 1984;25:97–110.
- Zechner R, Moser R, Newman T, Fried S, Breslow JL. Apolipoprotein E gene expression in mouse 3T3-L1 adipocytes and human adipose tissue and its regulation by differentiation and lipid content. *J Biol Chem* 1991;266:10583–8.
- Bustin SA. Absolute quantification of mRNA using real-time reverse transcription polymerase chain reaction assays [Review]. *J Mol Endocrinol* 2000;25:169–93.
- Emig M, Saussele S, Wittor H, Weisser A, Reiter A, Willer A, et al. Accurate and rapid analysis of residual disease in patients with CML using specific fluorescent hybridization probes for real time quantitative RT-PCR. *Leukemia* 1999;13:1825–32.
- Thellin O, Zorzi W, Lakaye B, De Borman B, Coumans B, Hennen G, et al. Housekeeping genes as internal standards: use and limits. *J Biotechnol* 1999;75:291–5.
- de Leeuw WJ, Slagboom PE, Vijg J. Quantitative comparison of mRNA levels in mammalian tissues: 28S ribosomal RNA level as an accurate internal control. *Nucleic Acids Res* 1989;17:10137–8.
- Nagel S, Schmidt M, Thiede C, Huhn D, Neubauer A. Quantification of Bcr-Abl transcripts in chronic myelogenous leukemia (CML) using standardized, internally controlled, competitive differential PCR (CD-PCR). *Nucleic Acids Res* 1996;24:4102–3.
- Rasmussen R. Quantification on the Light Cycle. In: Meuer S, Wittwer C, Nakagawara K, eds. *Rapid cycle real-time PCR: methods and applications*. Heilderberg: Springer Press, 2001:21–34.
- Finke J, Fritzen R, Ternes P, Lange W, Dölken G. An improved strategy and useful housekeeping gene for RNA analysis from formalin-fixed, paraffin-embedded tissues by PCR. *Biotechniques* 1993;14:448–53.
- Klucken J, Büchler C, Orsó E, Kaminski WE, Porsch-Özcürümez M, Liebisch G, et al. ABCG1 (ABC8), the human homolog of the *Drosophila* white gene, is a regulator of macrophage cholesterol and phospholipid transport. *Proc Natl Acad Sci U S A* 2000;97:817–22.
- Bhakdi S, Torzewski M, Klouche M, Hemmes M. Complement and atherogenesis: binding of CRP to degraded, nonoxidized LDL enhances complement activation. *Arterioscler Thromb Vasc Biol* 1999;19:2348–54.
- Klouche MA, May E, Hemmes M, Messner M, Kanse SM, Preissner KT, Bhakdi S. Enzymatically modified, nonoxidized LDL induces selective adhesion and transmigration of monocytes and T-lymphocytes through human endothelial cell monolayers. *Arterioscler Thromb Vasc Biol* 1999;19:784–93.
- Kraemer FB, Laane C, Park B, Sztalryd C. Low-density lipoprotein receptors in rat adipocytes: regulation with fasting. *Am J Physiol* 1994;266:E26–32.
- Prattes S, Horl G, Hammer A, Blaschitz A, Graier WF, Sattler W, et al. Intracellular distribution and mobilization of unesterified cholesterol in adipocytes: triglyceride droplets are surrounded by cholesterol-rich ER-like surface layer structures. *J Cell Sci* 2000;113:2977–89.